NASA TN D-4065

HEAT-TRANSFER MEASUREMENTS ON THE ROTOR BLADE OF A ROTOR ENTRY VEHICLE MODEL

By Ronald C. Smith and Alan D. Levin

Ames Research Center
Moffett Field, Calif.

NATIONAL AERONAUTICS AND SPACE ADMINISTRATION

For sale by the Clearinghouse for Federal Scientific and Technical Information
Springfield, Virginia 22151 – CFSTI price $3.00

HEAT-TRANSFER MEASUREMENTS ON THE ROTOR BLADE OF A ROTOR ENTRY VEHICLE MODEL

By Ronald C. Smith and Alan D. Levin

Ames Research Center

SUMMARY

Local heat transfer was measured on a rotor blade attached to a blunt body at a Mach number of 14 and total enthalpy of 4600 Btu/lb. Two ranges of angles of attack were investigated, one from 60° to 90° and another from 0° to 25°. Blade coning angle was varied from 0° to 45° with blade pitch angles of 0° and 10°.

The local heat transfer to blades in the body wake was found to be less than about half the reference heating rate (i.e., stagnation value on a hemisphere with a radius equal to the body radius). The heating rates increased rapidly in the vicinity of shock impingement; the maximum measured value was about eight times the reference heating rate. Heating rates were found to agree reasonably well with laminar theory in regions outboard of shock impingement at the high angles of attack (60° to 90°).

INTRODUCTION

A deployable rotor is one of many devices being examined as a means of modulating the lift and drag of a vehicle entering the earth's atmosphere. To derive the maximum range and deceleration control from lift and drag modulation, the rotor should be deployed as early as possible during the hypersonic phase of entry. It might be necessary, however, to delay deployment until after the highest rates of aerodynamic heating have been passed because, throughout entry, the heating rates of the blades are expected to be more severe than those of the body. It is therefore essential to know the local heating rates of the blades in detail in order to determine the highest speed at which the rotor can be safely deployed. The theoretical evaluation of blade heating rates is extremely difficult because of the nonuniform flow environment of rotor blades behind a blunt body, the bow shock impingement on the blades, and the separated wake from the body.

Shock impingement studies (refs. 1-3) indicate that for a cylinder with laminar flow, impingement of a plane oblique shock wave may triple the heating rates. It is suggested in reference 3 that the heating rate for turbulent flow might be used to predict the upper limit for the heating rate caused by shock impingement. Results of recent tests by Hiers and Loubsky (ref. 4) indicate that heating rates 10 or more times the laminar value can occur at the point of shock impingement on an airfoil with a blunt leading edge; in

these tests, the shock wave was generated by a flat plate with a sharp leading edge and the peak heating was highly localized.

Because of the uncertainties involved in predicting local blade heating rates, a series of heat-transfer tests were made in the Ames 1-Foot Shock Tunnel to measure heating rates on a rotor blade mounted on a blunt body. The present tests were intended to determine heating-rate distributions representative of the highest rates encountered by the blade in its path around the azimuth. For the low-angle-of-attack range, 0° to 25°, the 90° azimuth position was chosen and for the high-angle range, 60° to 90°, the 180° azimuth position was chosen. It is not expected that blade rotation would significantly modify the local heating rates at hypersonic speeds. It should be noted, however, that the temperature response of the blades of a rotor entry vehicle can be altered greatly by rotor rotation. For flight at angles of attack other than 90° (axial flight) where the body flow field is unsymmetrical, rotation will tend to spread the heat load from a localized region of shock-induced high heat flux over much of the blade surface. Consequently, to determine the blade temperature response additional tests are needed to determine how the heating-rate distribution changes around the azimuth.

NOTATION

$\dot{q}$	local heating rate, Btu/ft^2-sec
$\dot{q}_{hemi}$	stagnation heating rate on hemisphere, Btu/ft^2-sec
$\dot{q}_{ref}$	stagnation heating rate on hypothetical hemisphere having same radius as body heat shield, Btu/ft^2-sec
r/R	distance from body center line to thermocouple span station (in fractions of rotor radius)
U_∞	free-stream velocity, ft/sec
x/c	distance from blade leading edge to thermocouple chord station (in fractions of blade chord)
α	body angle of attack, deg
β	rotor coning angle, deg
θ	rotor blade pitch angle, deg
ψ	rotor blade azimuth angle, deg

MODEL DESCRIPTION

Bodies

Two bodies were constructed, one for the low-angle-of-attack range, 0° to 25°, and the other for the high-angle-of-attack range, 60° to 90°. The bodies were modified cones of 100° apex angle (fig. 1(a)) and were identical except for the location of the sting support. They were constructed of solid aluminum with polished surfaces. (Before each run, the front surface was carefully repolished.) Figures 1(b) and 1(c) show the configurations for the high- and low-angle-of-attack tests, respectively.

Blades

Two blades, one for each angle-of-attack range, were made with a stainless steel skin 0.008 inch thick attached to a steel support frame. Chromel-constantan thermocouples were induction welded to the inside of the blade skin at the spanwise and chordwise locations shown in figures 1(d) and 1(e). The blade for the high-angle model (fig. 1(b)) was attached to the sting and could be pitched independently of the model so that various combinations of angle of attack and coning angle could be tested. The blade for the low-angle model was attached directly to the body in a manner which permitted changes in the blade pitch angle. The surface of the blades was carefully polished before each run in order to insure, as nearly as possible, the same surface characteristics throughout the test.

Reference Hemisphere

A reference hemisphere of 0.5-inch radius was mounted on an auxiliary sting directly beneath the main model support sting as shown in figure 2. The reference hemisphere and model were separated sufficiently to insure a minimum of flow-field interaction, yet close enough for the flow impinging on the stagnation point of both the body and hemisphere to be the same. The hemisphere was formed from the same 0.008-inch stainless steel sheet from which the blades were constructed. A single chromel-constantan thermocouple was located at the stagnation point. The surface of the hemisphere was carefully polished before each run.

APPARATUS AND TEST CONDITIONS

The tests were conducted in the 1-Foot Shock Tunnel of the Ames Research Center. A full description of the tunnel and testing procedure used is given in references 5 and 6. The test conditions were as follows:

Total enthalpy	4600 Btu/lb
Free-stream entropy	2.27 Btu/lb-^{o}R
Free-stream velocity	13,200 ft/sec
Free-stream Mach number	14
Free-stream Reynolds number	71,000 ft^{-1}
Density altitude (ARDC)	164,000 ft
Test time	20 msec

RESULTS AND DISCUSSION

All heating-rate data were reduced to ratios of local heating rates to the stagnation-point heating rate on a hemisphere having the same radius as the body heat shield. The reference heating rate was obtained from the heating rate measured on the 0.5-inch radius hemisphere by making use of the relation

$$\dot{q}_{ref} = \dot{q}_{hemi} \left(\frac{1}{8}\right)^{1/2}$$

where 1/8 is the ratio of the radius of the hemisphere to the radius of the heat shield.

The heating-rate ratios as a function of r/R for various chordwise locations x/c are shown in figures 3 through 8.

High Angle of Attack

The results for the high angles of attack (60° to 90°) are shown in figures 3 to 5.

Wake heating.- The heating-rate ratios in the vicinity of the body wake are very low, about 0.2 to 0.6 for angles of attack of 75° and 90° and approximately 0.5 for an angle of attack of 60°. In the wake region the heating-rate ratios are essentially independent of coning angle at a fixed angle of attack.

Shock impingement.- Along the span of the blade there was a rapid rise in the heating rate close to the shock impingement point. The approximate locations of the impingement point of the body shock wave on the blade, as obtained from glow-discharge photographs, are indicated on figures 3 to 5. Results reported in reference 4 indicate that local heating rates at shock impingement can reach a value of 10 or more times the laminar value in an extremely localized area. For the present investigation the thermocouples

were not sufficiently close to insure measurement of the shock impingement heating rate. However, a very severe heating rate was measured at an angle of attack of 75° at 0° coning angle (fig. 4(a)). The heating-rate ratio was approximately 8, but was not located exactly at the shock impingement location noted in figure 4. Thus it cannot be stated that this value was actually the maximum. The heating-rate ratio of 8 corresponds to a heating rate 5.7 times the laminar value. The ratio of 10 reported in reference 4 was for a shock generated by a sharp leading edge impinging a cylindrical leading edge.

Outboard of shock impingement.- For angles of attack of 75° and 60° (figs. 4 and 5, respectively), the heating-rate ratio agrees reasonably well with the laminar heat-transfer theory developed in reference 7. The heating-rate ratios predicted by laminar theory are for a two-dimensional cylinder of radius equal to the maximum radius of curvature of the blade and inclined at an angle $(\beta - \alpha)$ to the free stream. Outboard of the shock impingement the heating-rate ratios vary from about 1.4 to 1.8 for $x/c = 0.5$, depending upon angle of attack and coning angle. For the condition of axial flight $\alpha = 90^\circ$ (fig. 3(a)) the heating-rate ratio for a coning angle of 0° agrees reasonably well with the value of 1.5 predicted by laminar theory. For coning angles of 30° and 45° (figs. 3(b) and (c)) there was essentially no region on the blade which could be considered outboard of the shock impingement. At a coning angle of 30° the shock impingement occurred in the vicinity of the most outboard thermocouple, as indicated by the rise in heating rate at that point. At a coning angle of 45° the rotor blade was entirely within the shock envelope generated by the body. The heating-rate ratios in this case were about 0.6 and were essentially constant in both the spanwise and chordwise directions.

Low Angle of Attack

The results for the low-angle-of-attack range (0° to 25°) are presented in figures 6 to 8. Only the azimuth position $\psi = 90^\circ$ was tested since it was expected to produce the most severe heating condition. The heating rates for azimuth angles other than 90° may be estimated, at least on the portion of the blade outboard of shock impingement, by making use of the known effects of sweep on the aerodynamic heating, as indicated in references 8 and 9.

Leading-edge heating.- The heating-rate ratios in the vicinity of the leading edge varied from about 4.0 to 5.0 (flagged symbols in figs. 6, 7, and 8). This was about half the value (11.0) predicted by laminar theory for $\alpha = 0^\circ$, $\theta = 0^\circ$ (fig. 8). The reason for the large difference between experiment and theory probably lies with the limitation of the instrumentation to record the leading-edge heating rates. For the present tests, the blade leading-edge radius of 0.017 inch was too small for the skin thickness of 0.008 inch. The small radius caused the leading-edge thermocouples to be heavily influenced by the entire region near the leading edge and therefore to record only the average heating rate over this region.

Shock impingement.- For the 0° to 25° angle-of-attack range the shock impingement point remains inboard of the $r/R = 0.333$ spanwise station.

Because of the limited instrumentation in this region, a definite shock impingement point was not located. However, at 0° angle of attack and 0° blade pitch (fig. 8) a heating-rate ratio between 7 and 8 was obtained. Approximately the same value was also obtained at 15° angle of attack and 10° of blade pitch (fig. 7). In relation to the other values along the span they indicate that a shock impingement point was being approached.

Outboard of shock impingement.- The local heating-rate ratios along the blade midchord line are low, being less than 1.0 in most instances. Generally there was an increase in the midchord heating as the blade inclination to the stream ($\alpha + \theta$) was increased.

CONCLUSIONS

The following general conclusions are drawn as a result of the investigation:

1. In the angle-of-attack range from 60° to 90° the blade heating rates in the wake are low, reaching a maximum value of about 0.6 times the reference heating rate, and, for a given angle of attack, are essentially independent of coning angle. (The reference heating rate represents the stagnation-point heating on a hypothetical hemisphere having a radius equal to the body heat-shield radius.)

2. The heating rates at shock impingement reach a value of at least eight times the reference heating rate. The region of severe heating due to shock impingement is highly localized.

3. Outboard of the shock impingement region the heating rates agree reasonably well with the theoretical values predicted by laminar theory.

4. In the angle-of-attack range from 0° to 25°, the leading-edge heating rates were approximately half the value predicted by laminar theory. Because the leading-edge radius was too small for the skin thickness, it is believed that the heat-transfer rates measured at the leading edge represent an average value for the entire region near the leading edge.

5. At low angles of attack the heating rates along the blade midchord line were generally less than the reference heating rate. The midchord heat-transfer rates were found to increase with increasing blade inclination.

Ames Research Center
National Aeronautics and Space Administration
Moffett Field, Calif., 94035, April 28, 1967
124-07-03-04-00-21

REFERENCES

1. Siler, L. G., et al.: Effect of Shock Impingement on the Heat-Transfer and Pressure Distributions on a Cylindrical-Leading-Edge Model at Mach Number 19. AEDC-TDR-64-228, ARO, Inc., Nov. 1964.

2. Newlander, Robert A.: Effect of Shock Impingement on the Distribution of Heat-Transfer Coefficients on a Right Circular Cylinder at Mach Numbers of 2.65, 3.51, and 4.44. NASA TN D-642, 1961.

3. Jones, Robert A.: Heat-Transfer and Pressure Investigation of a Fin-Plate Interference Model at a Mach Number of 6. NASA TN D-2028, 1964.

4. Hiers, Robert S.; and Loubsky, William J.: Effects of Shock-Wave Impingement on the Heat Transfer on a Cylindrical Leading Edge. NASA TN D-3859, 1967.

5. Cunningham, Bernard E.; and Kraus, Samuel: A 1-Foot Hypervelocity Shock Tunnel in Which High-Enthalpy, Real-Gas Air Flows Can be Generated With Flow Times of About 180 Milliseconds. NASA TN D-1428, 1962.

6. Loubsky, William J.; Hiers, Robert S.; and Stewart, David A : Performance of a Combustion Driven Shock Tunnel With Application to the Tailored-Interface Operating Conditions. Presented at Third Conf. on Performance of High Temperature Systems, 1964.

7. Lees, Lester: Laminar Heat Transfer Over Blunt-Nosed Bodies at Hypersonic Flight Speeds. Jet Propulsion, vol. 26, no. 4, April 1956, pp. 259-269.

8. Horstman, C. C.; and Vas, I. E.: The Flow About the Leading Edge of a Swept Blunt Plate at Hypersonic Speeds. Princeton Univ. Report 616, June 1962.

9. Wisniewski, Richard J.: Methods of Predicting Laminar Heat Rates on Hypersonic Vehicles. NASA TN D-201, 1959.

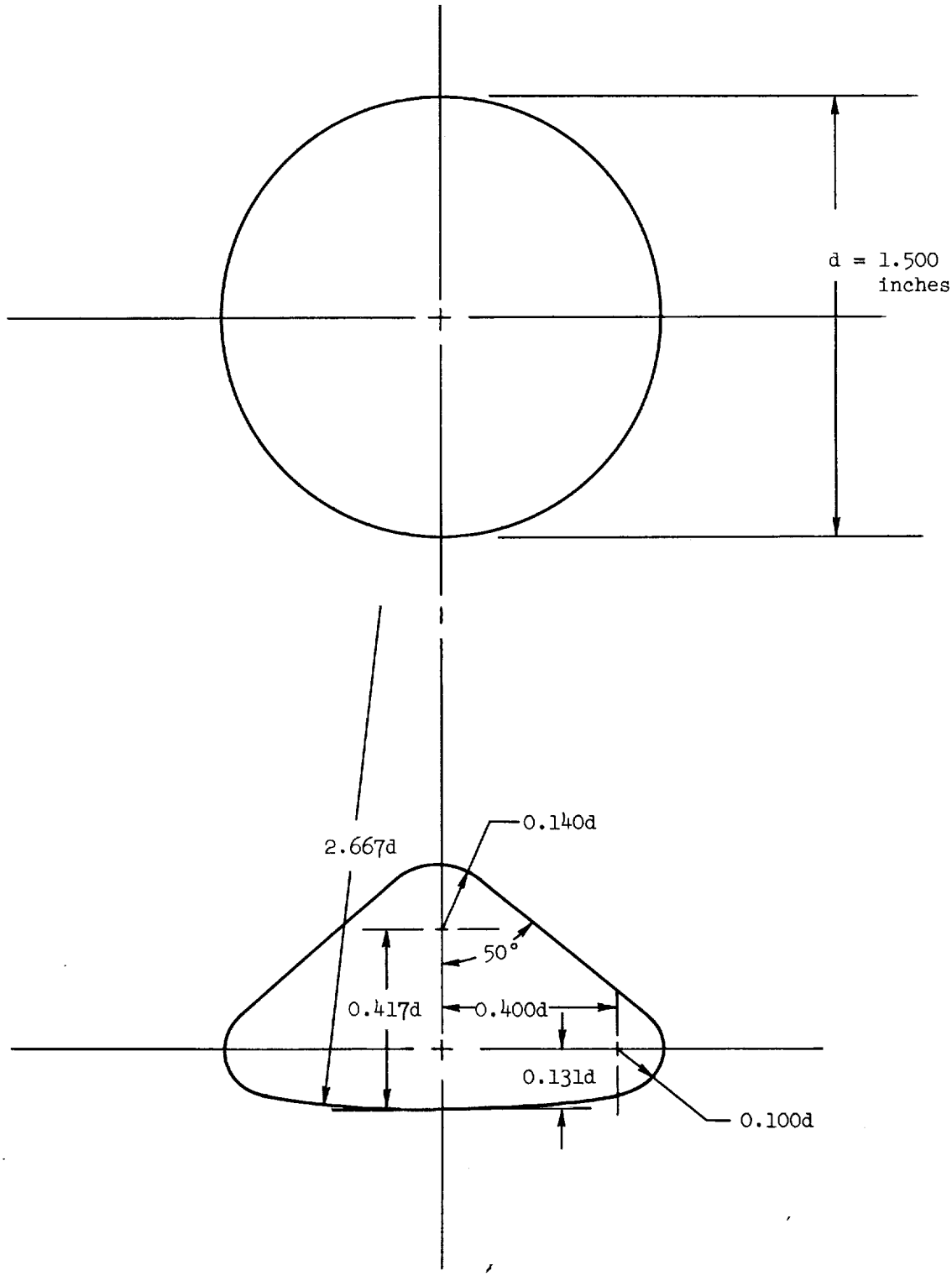

(a) Body

Figure 1.- Model details.

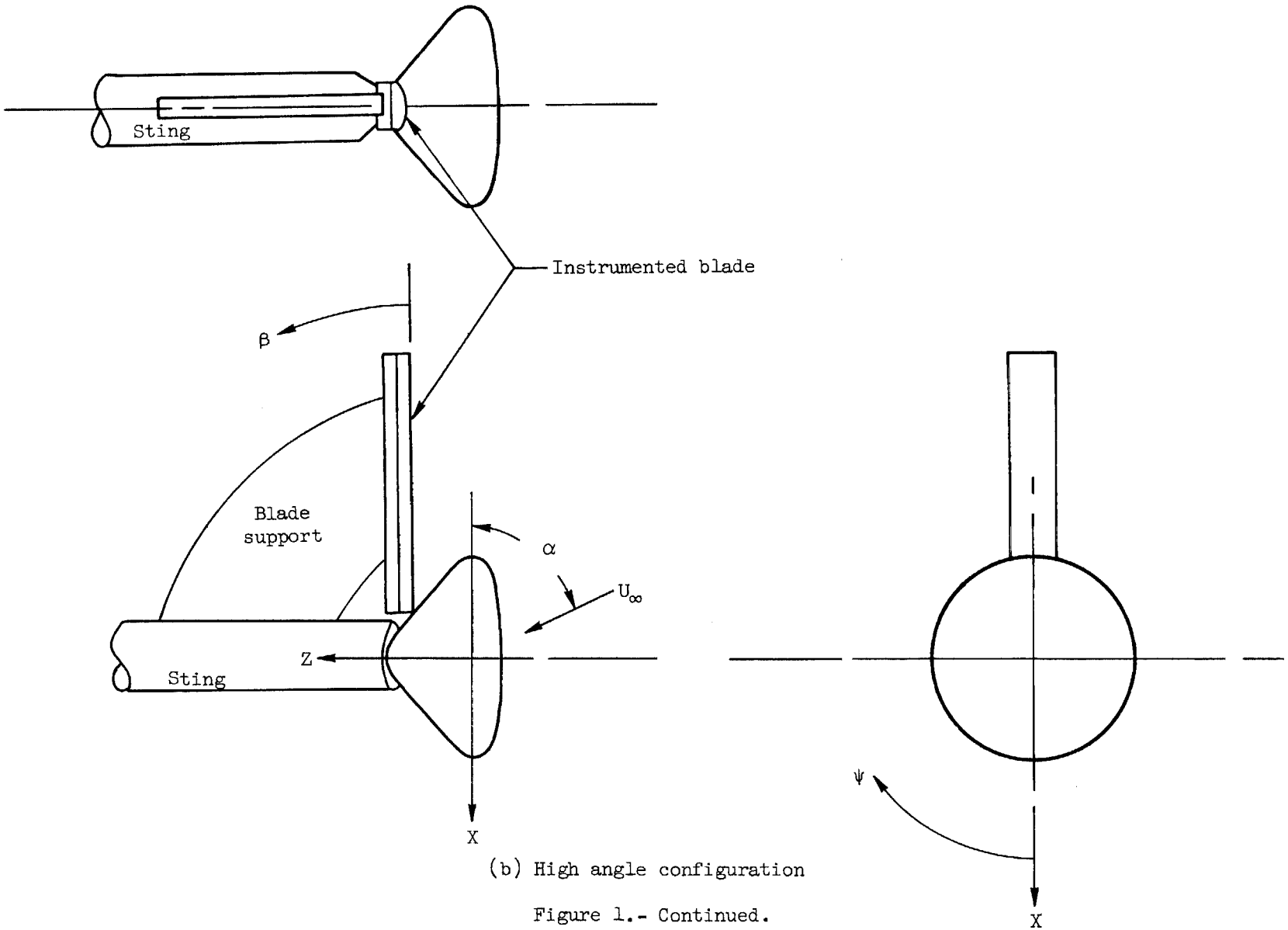

(b) High angle configuration

Figure 1.- Continued.

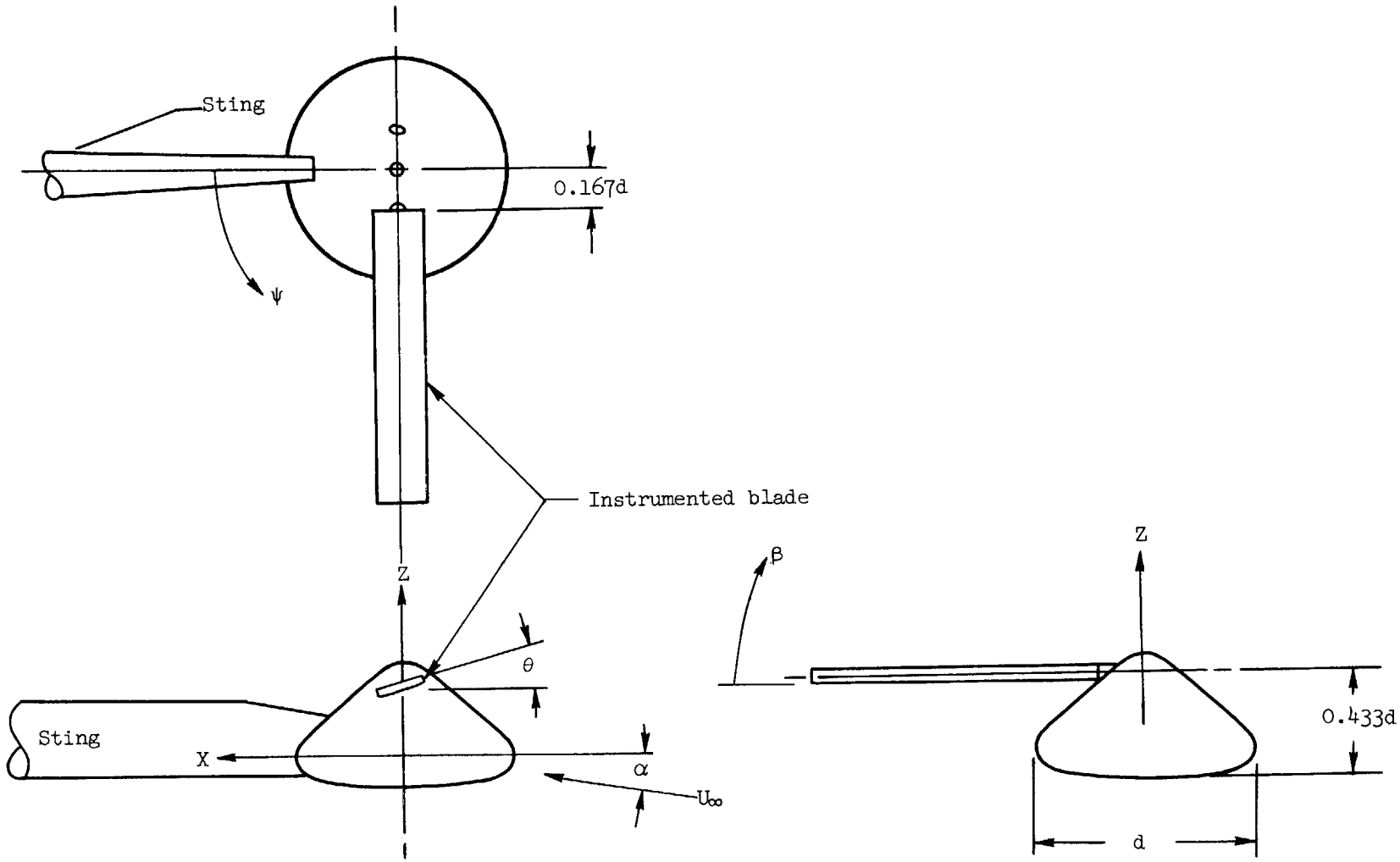

(c) Low angle configuration

Figure 1.- Continued.

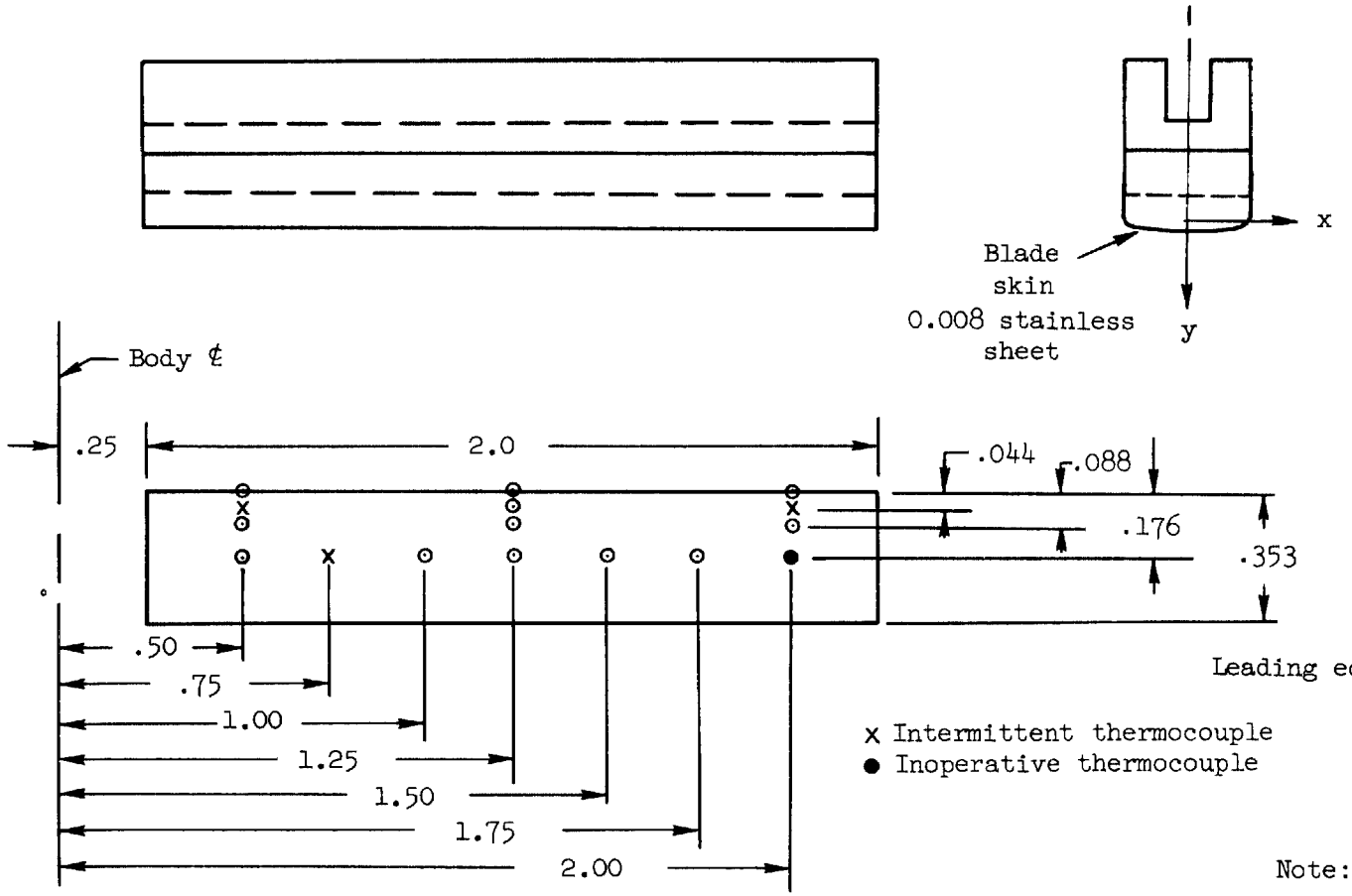

BLADE SECTION COORDINATES

± x/c	y/c
0.0000	0.1000
0.0417	0.0994
0.0834	0.0985
0.1250	0.0969
0.1667	0.0950
0.2083	0.0925
0.2500	0.0890
0.2917	0.0840
0.3333	0.0777
0.3750	0.0702
0.4167	0.0606
0.4583	0.0481
0.4688	0.0440
0.4792	0.0388
0.4896	0.0299

Leading edge radius = 0.0469c

Note: All dimensions are in inches

(d) Blade geometry, high angle configuration

Figure 1.- Continued.

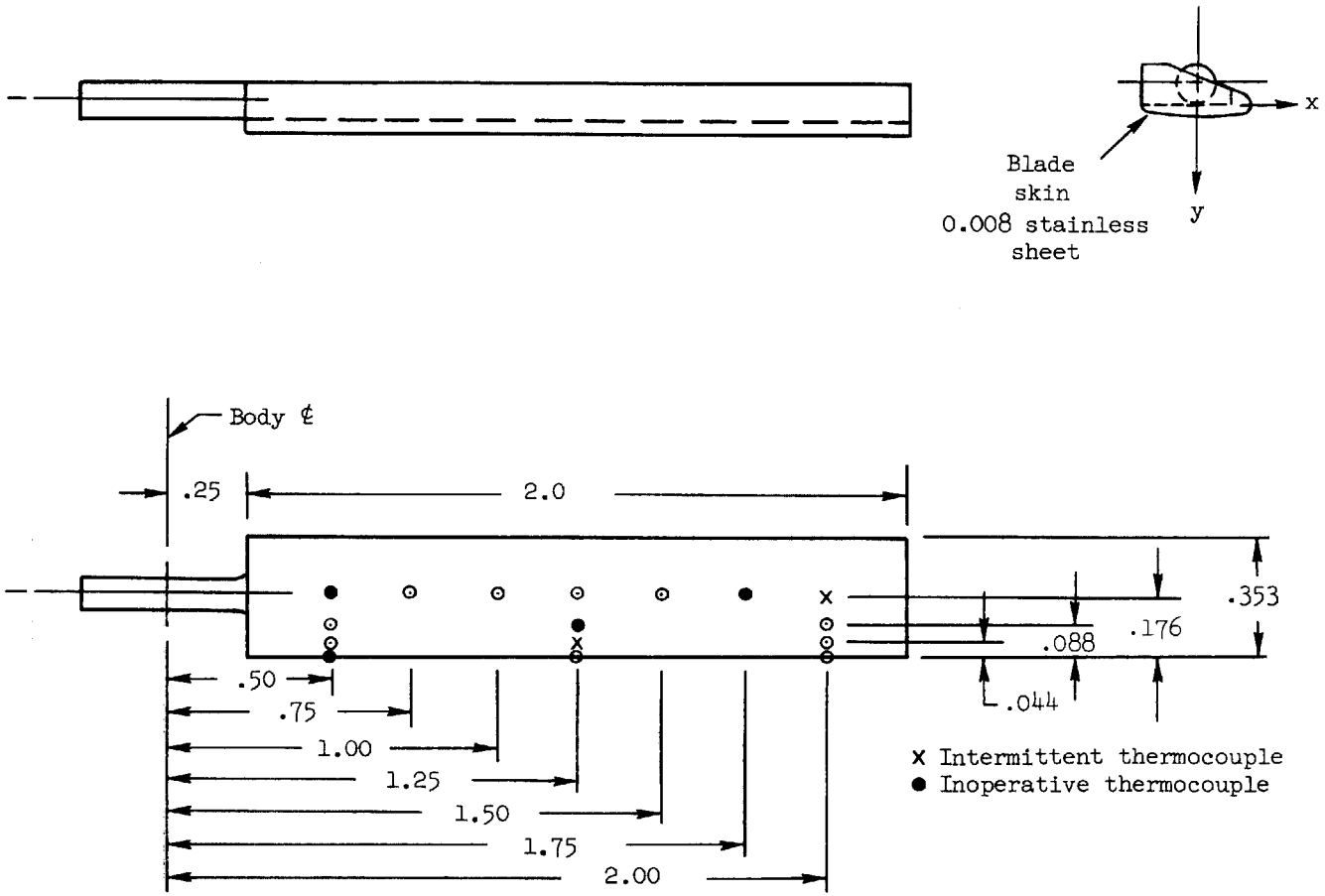

BLADE SECTION COORDINATES

± x/c	y/c
0.0000	0.1000
0.0417	0.0994
0.0834	0.0985
0.1250	0.0969
0.1667	0.0950
0.2083	0.0925
0.2500	0.0890
0.2917	0.0840
0.3333	0.0777
0.3750	0.0702
0.4167	0.0606
0.4583	0.0481
0.4688	0.0440
0.4792	0.0388
0.4896	0.0299

Leading edge radius = 0.0469c

Note: All dimensions are in inches

(e) Blade geometry, low angle configuration

Figure 1.- Concluded.

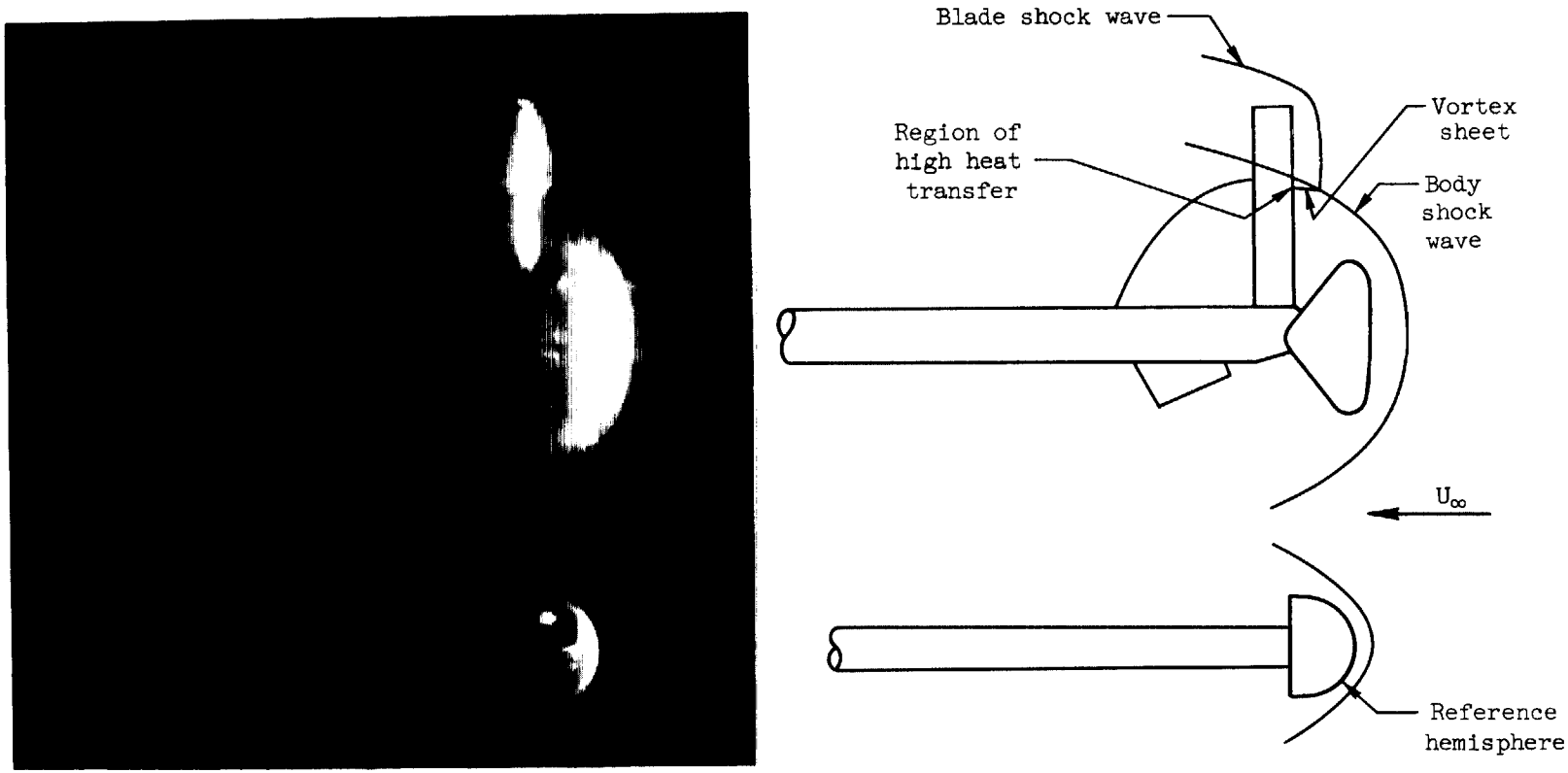

Figure 2.- Glow discharge photograph. Sketch shows important features of the flow; $\alpha = 90°$, $\beta = 0°$.

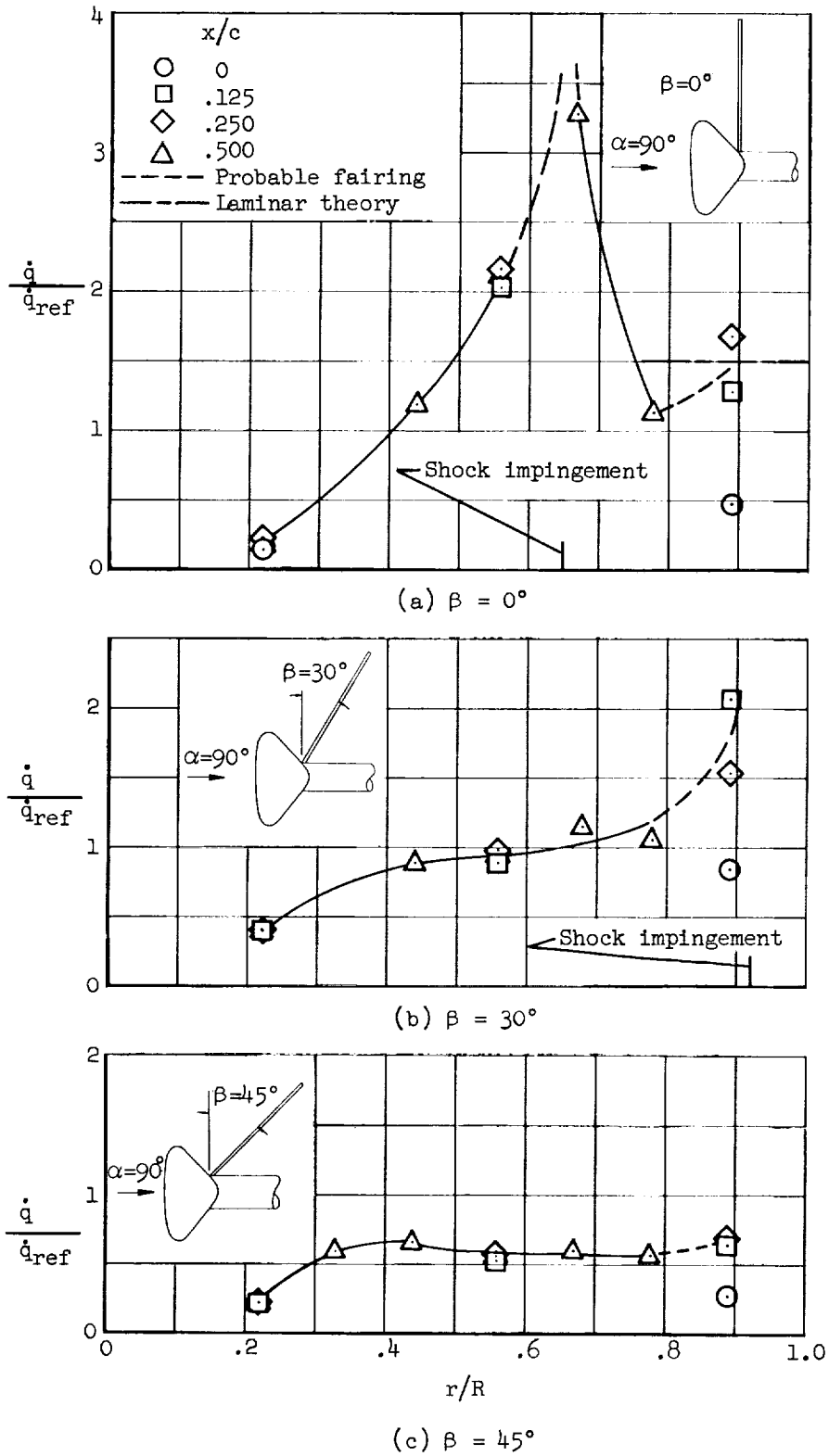

Figure 3.- Rotor-blade heating-rate distributions for three coning angles; $\alpha = 90°$.

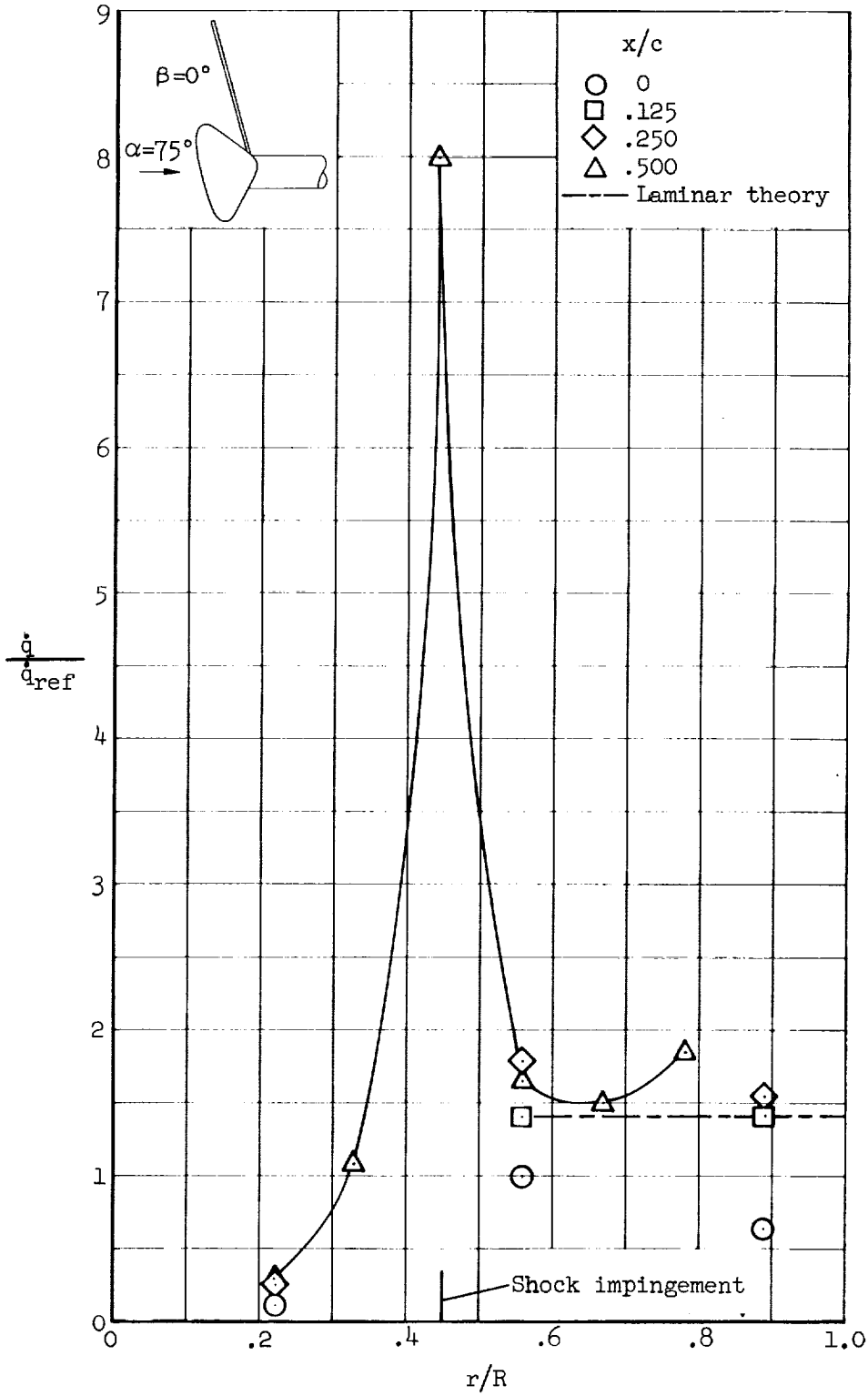

(a) $\beta = 0°$

Figure 4.- Rotor-blade heating-rate distribution; $\alpha = 75°$.

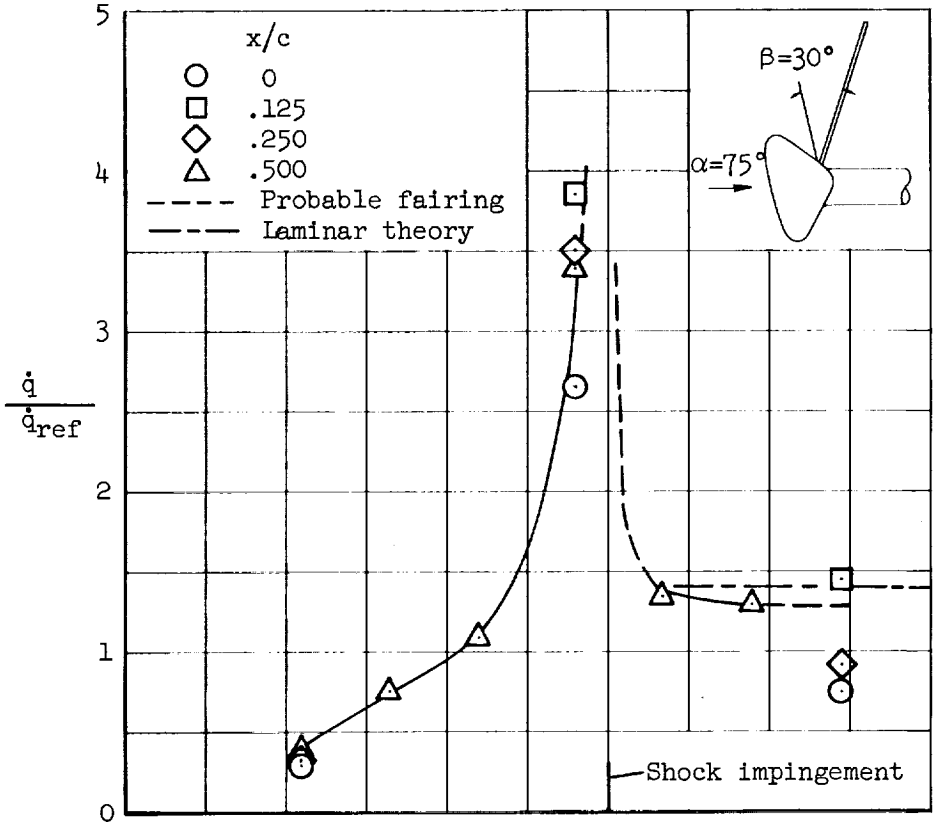

(b) β = 30°

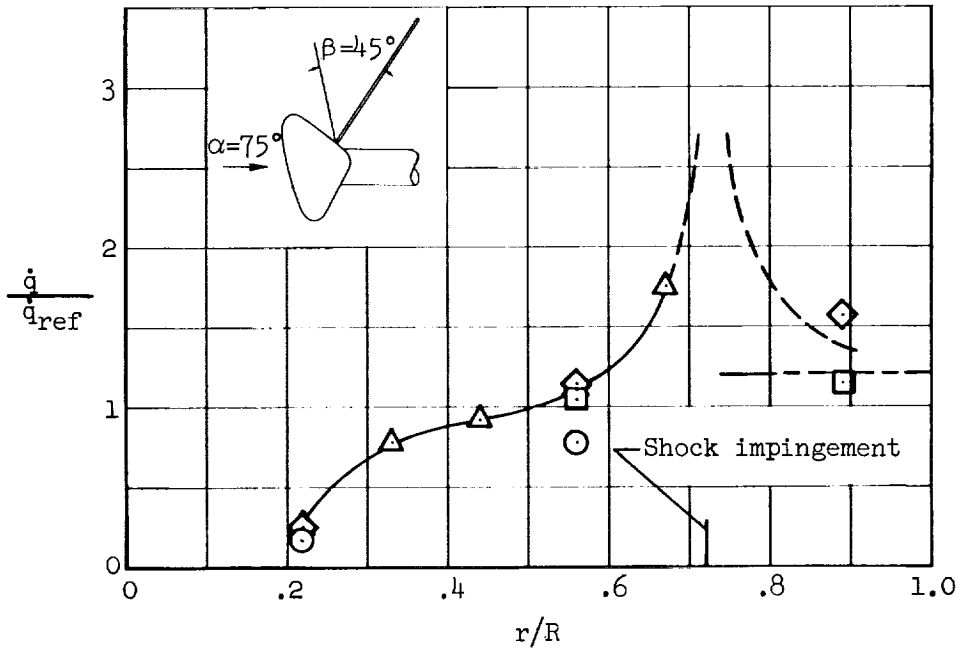

(c) β = 45°

Figure 4.- Concluded.

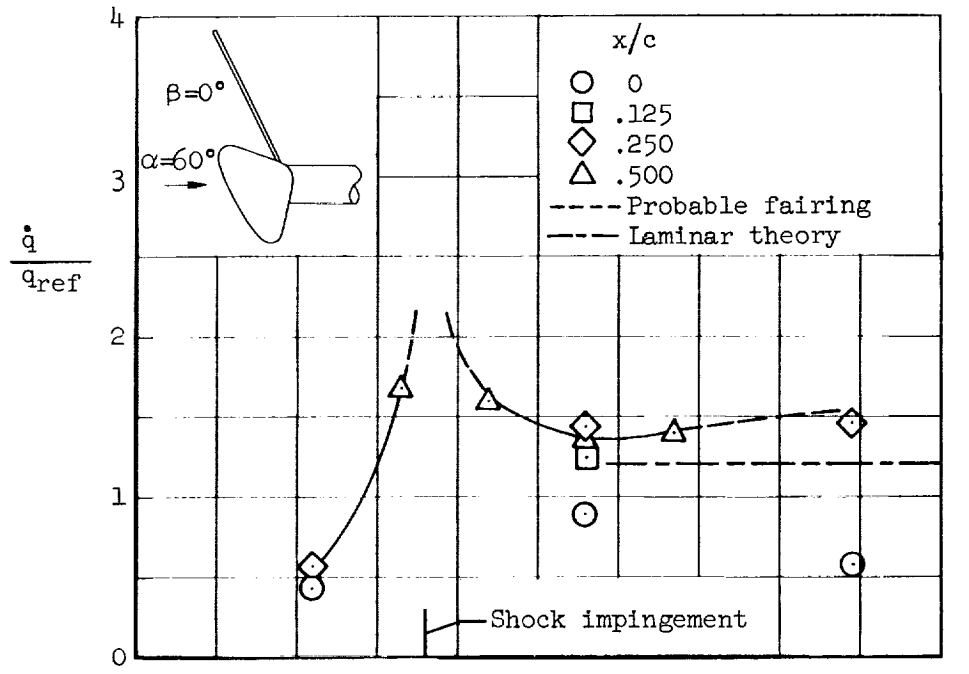

(a) β = 0°

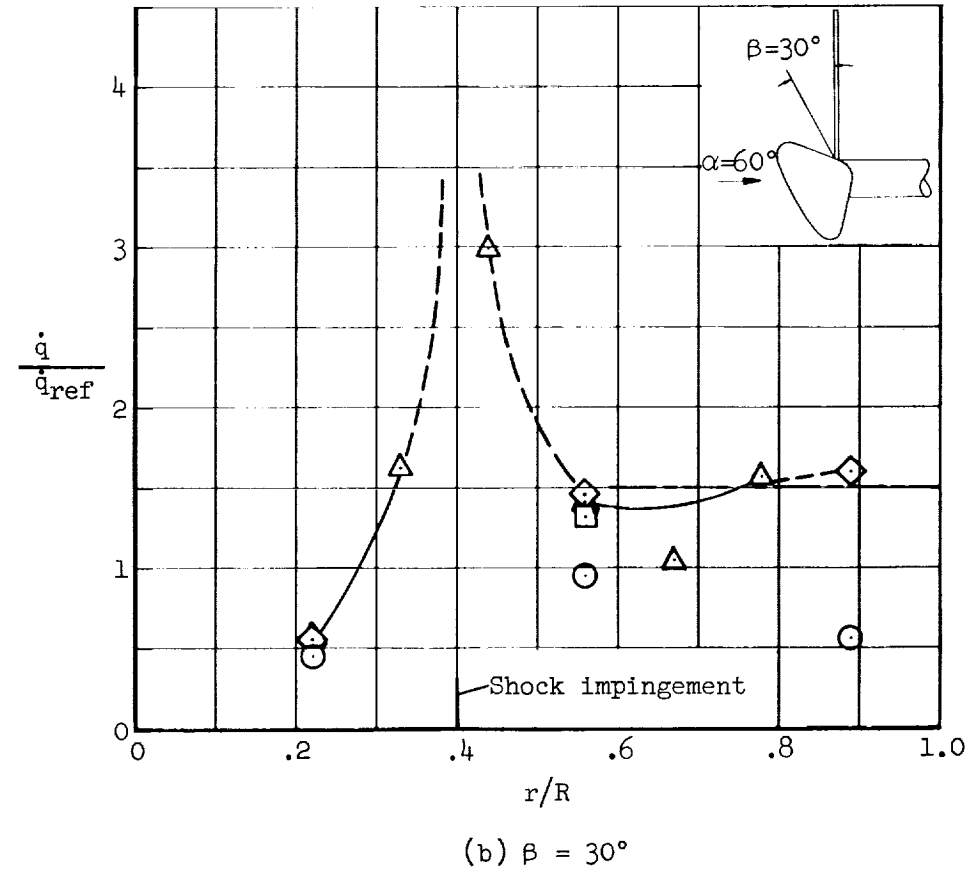

(b) β = 30°

Figure 5.- Rotor-blade heating-rate distributions; α = 60°.

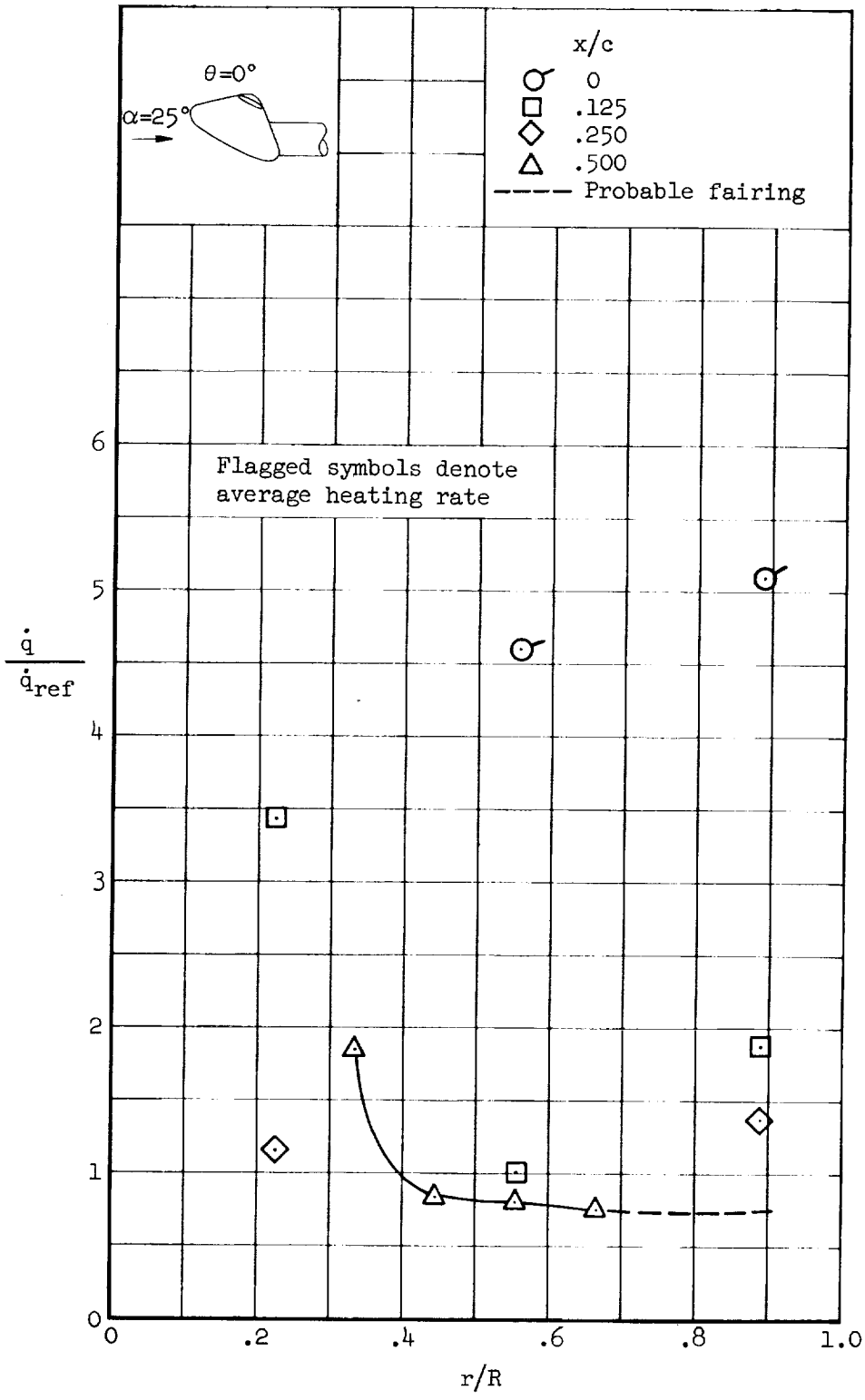

(a) $\theta = 0°$

Figure 6.- Rotor-blade heating-rate distributions for $\alpha = 25°$; $\psi = 90°$.

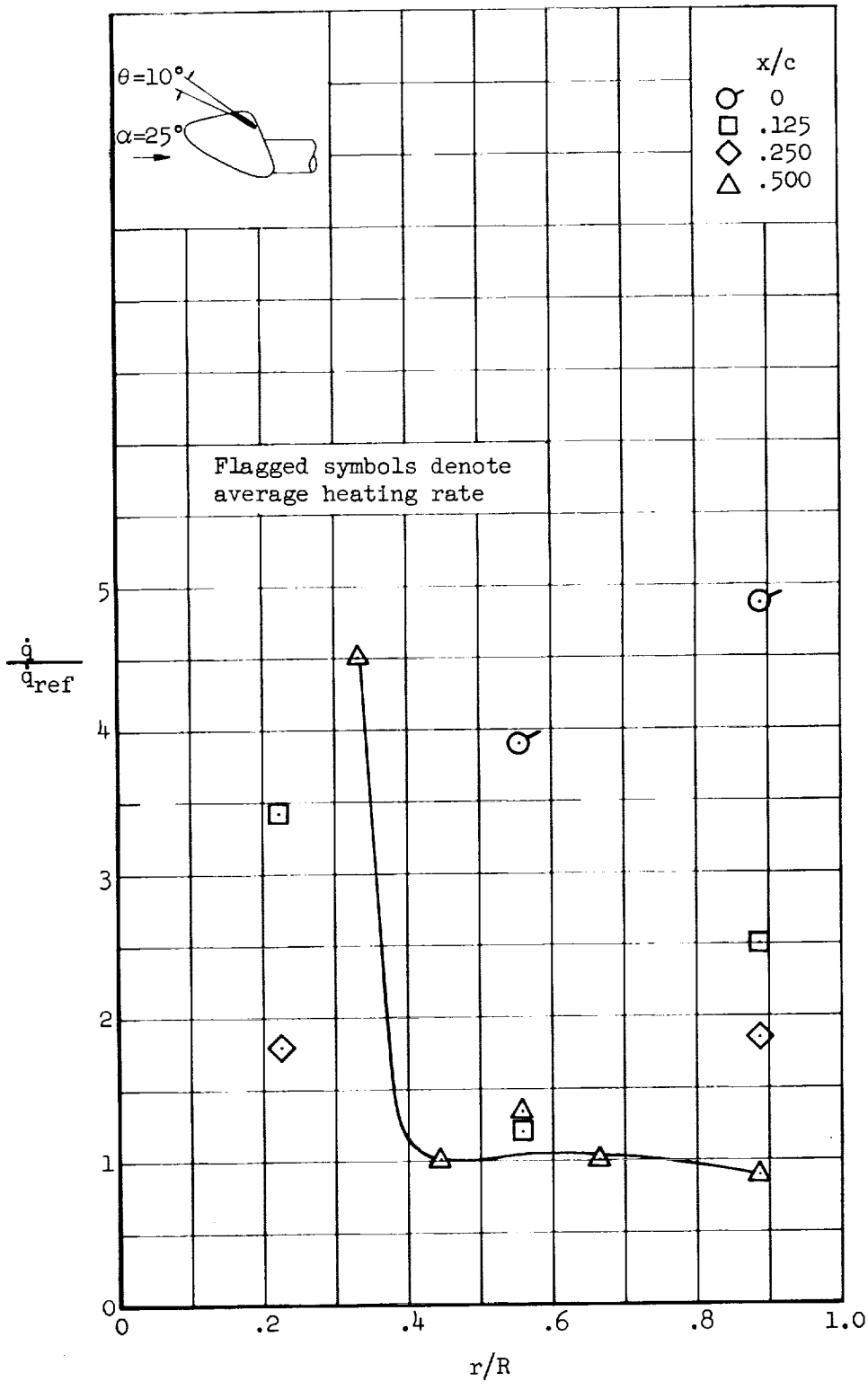

(b) θ = 10°

Figure 6.- Concluded.

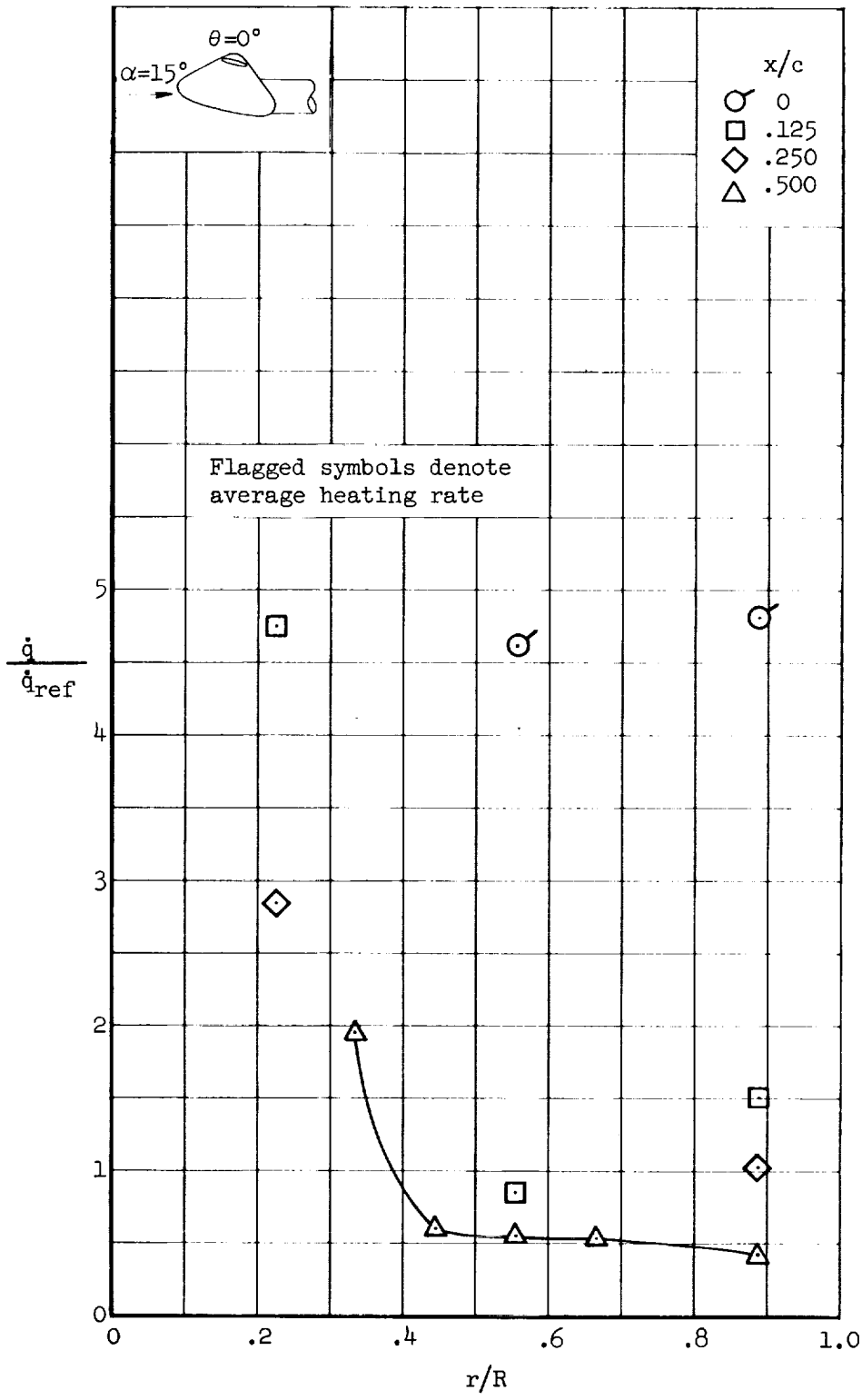

(a) $\theta = 0°$

Figure 7.- Rotor-blade heating-rate distributions for $\alpha = 15°$; $\psi = 90°$.

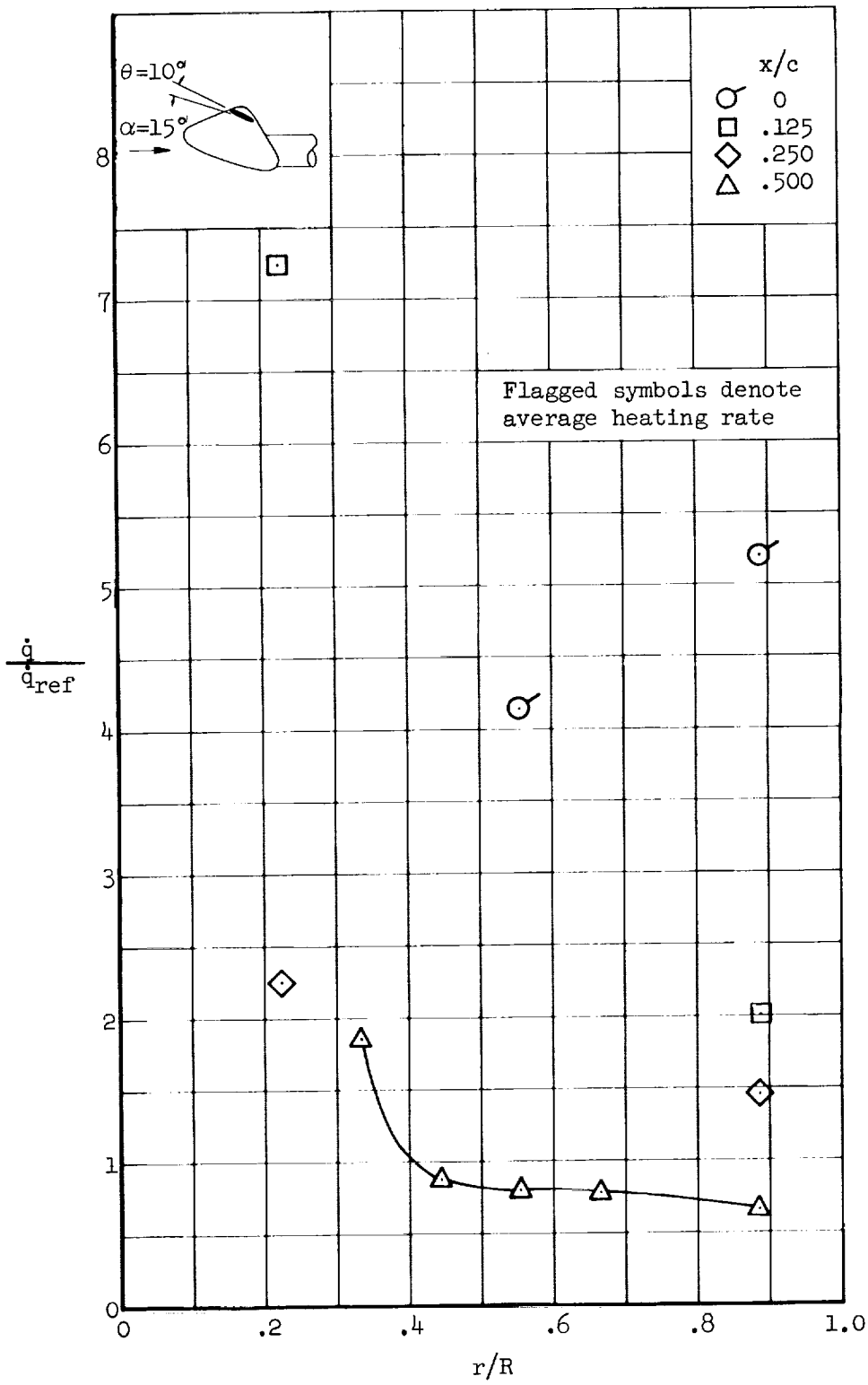

(b) θ = 10°

Figure 7.- Concluded.

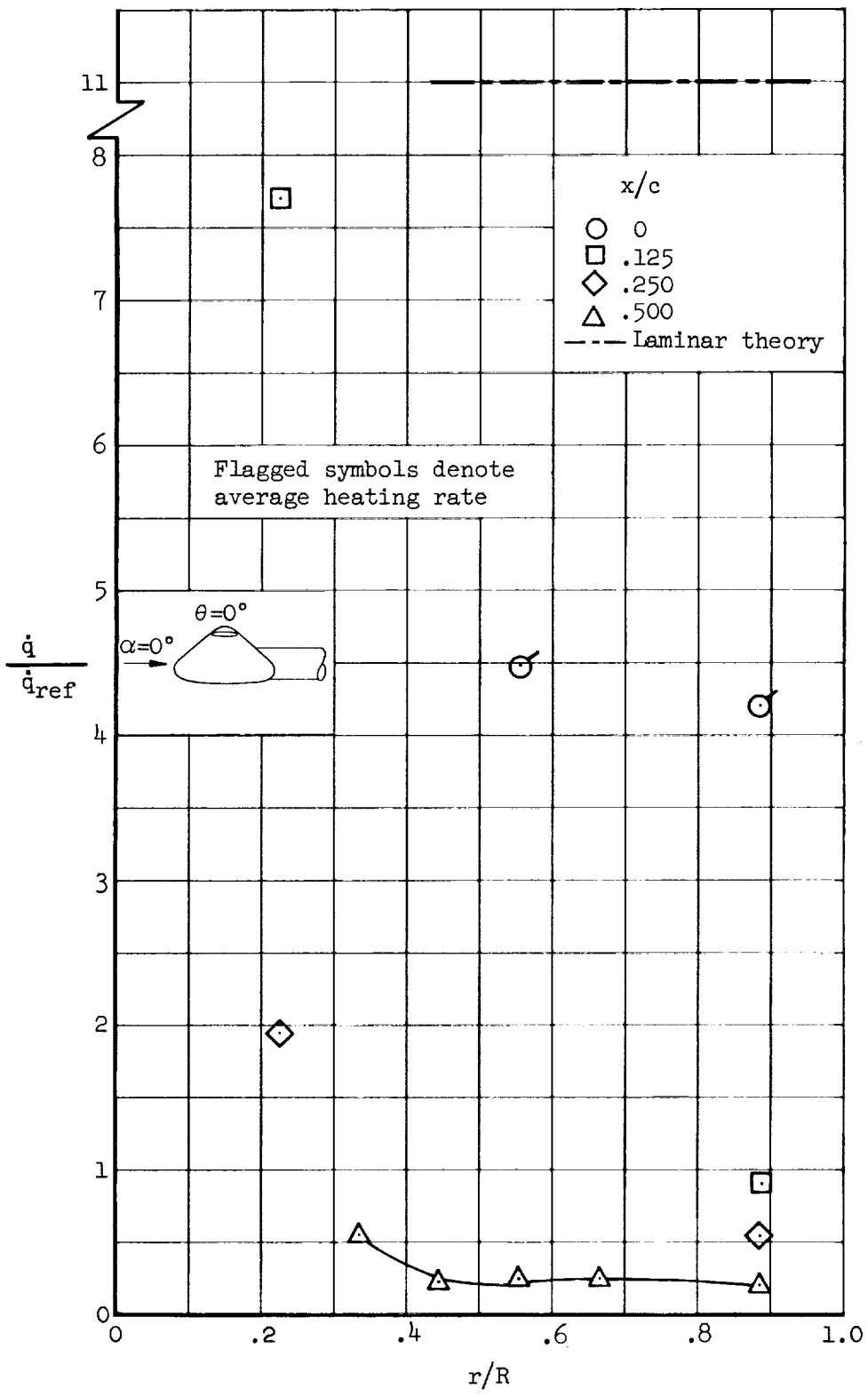

Figure 8.- Rotor-blade heating-rate distributions for $\alpha = 0°$; $\psi = 90°$.